# Characterization of cellular, biochemical and genomic features of the diazotrophic plant growth-promoting bacterium *Azospirillum* sp. UENF-412522, a novel member of the *Azospirillum* genus

Gustavo L. Rodrigues[a,*], Filipe P. Matteoli[a,*], Rajesh K. Gazara[a], Pollyanna S. L. Rodrigues[b], Samuel T. dos Santos[b], Alice F. Alves[b,c], Francisnei Pedrosa-Silva[a], Isabella Oliveira-Pinheiro[a], Daniella Canedo-Alvarenga[a], Fabio L. Olivares[b,c,#], Thiago M. Venancio[a,#]

[a] Laboratório de Química e Função de Proteínas e Peptídeos, Centro de Biociências e Biotecnologia, Universidade Estadual do Norte Fluminense Darcy Ribeiro (UENF), Brazil; [b] Núcleo de Desenvolvimento de Insumos Biológicos para a Agricultura (NUDIBA), UENF, Brazil; [c] Laboratório de Biologia Celular e Tecidual, Centro de Biociências e Biotecnologia, UENF, Brazil. [*] Contributed equally to this work.

[#] **Corresponding authors:**
Thiago M. Venancio; Laboratório de Química e Função de Proteínas e Peptídeos, Centro de Biociências e Biotecnologia, UENF; Av. Alberto Lamego 2000, P5 / sala 217; Campos dos Goytacazes, Rio de Janeiro, Brazil. E-mail: thiago.venancio@gmail.com.

Fabio L. Olivares: Laboratório de Biologia Celular e Tecidual, Centro de Biociências e Biotecnologia, UENF, Brazil. E-mail: fabioliv@uenf.br.

**ABSTRACT**

Given their remarkable beneficial effects on plant growth, several *Azospirillum* isolates currently integrate the formulations of various commercial inoculants. Our research group isolated a new strain, *Azospirillum* sp. UENF-412522, from passion fruit rhizoplane. This isolate uses carbon sources that are partially distinct from closely-related *Azospirillum* isolates. Scanning electron microscopy analysis and population counts demonstrate the ability of *Azospirillum* sp. UENF-412522 to colonize the surface of passion fruit roots. *In vitro* assays demonstrate the ability of *Azospirillum* sp. UENF-412522 to fix atmospheric nitrogen, to solubilize phosphate and to produce indole-acetic acid. Passion fruit plantlets inoculated with *Azospirillum* sp. UENF-41255 showed increased shoot and root fresh matter, as well as root dry matter, further highlighting its biotechnological potential for agriculture. We sequenced the genome of *Azospirillum* sp. UENF-412522 to investigate the genetic basis of its plant-growth promotion properties. We identified the key *nif* genes for nitrogen fixation, the complete PQQ operon for phosphate solubilization, the *acdS* gene that alleviates ethylene effects on plant growth, and the *napCAB* operon, which produces nitrite under anoxic conditions. We also found several genes conferring resistance to common soil antibiotics, which are critical for *Azospirillum sp.* UENF-412522 survival in the rhizosphere. Finally, we also assessed the *Azospirillum* pangenome and highlighted key genes involved in plant growth promotion. A phylogenetic reconstruction of the genus was also conducted. Our results support *Azospirillum sp.* UENF-412522 as a good candidate for bioinoculant formulations focused on plant growth promotion in sustainable systems.

## INTRODUCTION

Modern agriculture production strongly relies on synthetic fertilizers and pesticides to achieve high productivity levels, which are often a matter of environmental and health concerns [1]. The development of bioinoculants has been considered an alternative to reduce the use of such synthetic compounds [2]. These inoculants typically have one or more strains of plant growth-promoting rhizobacteria (PGPR), which compose a heterogeneous group of bacteria that exert mutualistic interactions with plants [3], often playing key roles in the root microbiome [4]. The rhizosphere is the fraction of soil directly influenced by roots exudates [5], which modulate bacterial diversity across the endorhizosphere, rhizoplane and ectorhizhosphere (reviewed by Ahkami et al. [6]). Several *Azospirillum* isolates have been reported as PGPR, typically as soil-borne bacteria that are competent rhizosphere colonizers [7, 8].

The genus *Azospirillum* belongs to the *Rhodospirillaceae* family, which is mainly constituted of aquatic genera. Nevertheless, Azospirilla are mostly soil bacteria that coevolved with vascular plants [9]. Following its original description [10], multiple plant-associated *Azospirillum* species have been shown to perform direct nitrogen fixation [11, 12], phosphate solubilization [13], drought and salt stress alleviation [14, 15], root development promotion [16], among other processes [17]. These desirable properties have led several *Azospirillum* strains to be used as part of commercial soil inoculants [18]. Genes associated with these features have been identified in several publicly available *Azospirillum* genomes, such as *nif* [19], ACC-deaminase (*acds*) [20, 21], *pqq* [22], and indole acetic acid biosynthesis genes (e.g., *iaaH*, *iaaM* and *ipdC*) [23, 24].

Recently, our research group has isolated several plant growth-promoting bacterial strains from vermicompost [25, 26] and from the rhizosphere of tropical fruit trees. Among these strains, *Azospirillum sp.* UENF-412522 was isolated from passion fruit rhizoplane. Here we report *in vitro* and *ex vitro* plant growth promotion capabilities, biochemical tests, microscopy analysis of root colonization, whole-genome sequencing, and comparative genomic analyses to investigate the plant growth promotion properties of this isolate, as well as to uncover genes involved in other ecophysiological processes. Together, our results support the potential of *Azospirillum sp.* UENF-412522 to be used in bioinoculant formulations.

## RESULTS AND DISCUSSION

### Identification of the isolate and assessment of plant growth promotion properties

The strain UENF-412522 was isolated from passion fruit rhizoplane and formed a pellicle typical of diazotrophic bacteria on N-free semisolid NFb medium. It is a Gram negative, slightly curved rod-shaped bacterium with apparently no polymorphic 1.2 x 0.7 µm cells. In order to characterize the isolated strain, a fragment of the 16S rDNA gene was amplified by polymerase chain reaction (PCR); this sequence was deposited in Genbank under the accession KU836626.1. The 16S rDNA maximum likelihood (ML) phylogenetic reconstruction (Figure S1) has not allowed us to classify the strain at the species level. Nevertheless, it is clear that it belongs to the *Azospirillum* genus, leading us to name it *Azospirillum sp.* UENF-412522.

Given the evidence supporting *Azospirillum* sp. UENF-412522 as a novel *Azospirillum* species, we used an API 50 CH system and found that it grows on 18 out of 49 tested carbon sources: glycerol, D-arabinose, L-arabinose, D-ribose, D-xylose, methyl-beta-D-xylopyranoside, D-galactose, D-glucose, D-fructose, D-mannose, L-sorbose, amygdalin, aesculin ferric citrate, D-

90 melibiose, glycogen, xylitol, D-xylose, D-fucose. On the other hand, this strain was unable to
91 grow on: erythritol, L-xylose, D-adonitol, L-rhamnose, dulcitol, inositol, D-mannitol, D-sorbitol,
92 Methyl-alpha-D-mannopyranoside, Methyl-alpha-D-glucopyranoside, N-acetylglucosamine,
93 arbutin, salicin, D-cellobiose, D-maltose, D-lactose (bovine origin), D-saccharose (sucrose), D-
94 trehalose, inulin, D-melezitose, D-raffinose, amidon (starch), gentiobiose, D-turanose, D-
95 tagatose, L-fucose, D-arabitol, L-arabitol, potassium gluconate, potassium 2-ketogluconate,
96 potassium 5-ketogluconate. Comparison of carbon utilization patterns of *Azospirillum* sp. UENF-
97 412522 and those of the type strains of *Azospirillum lipoferum* ATCC 29707 [10], *Azospirillum*
98 *doebereinerae* DSM 13131 [27] and *Azospirillum brasilense* ATCC 29145 showed that four C-
99 sources (i.e. D-ribose, D-mannitol, D-sorbitol and N-acetylglucosamine) could be used to
100 discriminate these isolates (Table S1).
101 Next, we performed *in vitro* tests that would account for the ability of *Azospirillum* sp.
102 UENF-412522 to promote plant growth. The $N_2$-fixation was supported by positive growth on N-
103 free semisolid medium and subsequently confirmed by the amplification of *nifH* (Figure 1A). We
104 also confirmed the nitrogenase activity by using the acetylene reduction assay, which showed a
105 rate of 28.3 $\pm$ 5.1 nmol.h$^{-1}$ ethylene (Figure 1B).
106 Indole-acetic acid (IAA) production was investigated in DYGS medium, with and without
107 L- tryptophan, resulting in IAA concentrations of 51.34 $\pm$ 1.1 µg.mL$^{-1}$ and 37.35 $\pm$ 3.5 µg.mL$^{-1}$,
108 respectively (Figure 1C), supporting the capacity of *Azospirillum* sp. UENF-412522 to synthesize
109 this important plant hormone.
110 We also tested whether *Azospirillum* sp. UENF-412522 is able to solubilize Araxá P-rock
111 and calcium phosphate in solid medium. We found that this strain formed a halo with a
112 solubilization index (SI) of 3.33 $\pm$ 0.05 and 1.87 $\pm$ 0.11 for Araxá P-rock and calcium phosphate,
113 respectively (Figure 1D). We confirmed the P solubilization activity using a liquid medium assay,
114 which showed 147.5 $\pm$ 3.9 mg.L$^{-1}$ and 52.2 $\pm$ 8.6 mg.L$^{-1}$ solubilized P from Araxá P-rock and
115 calcium phosphate (Figure 1E), respectively. Conversely, zinc solubilization was not detected,
116 likely because of zinc sensitivity in this strain.
117 The plant growth-promoting effects of a given bacterial strain often result from several
118 concerted processes. Therefore, we inoculated passion fruit plantlets with *Azospirillum* sp.
119 UENF-412522 and found a clear growth increment in inoculated versus non-inoculated plantlets.
120 After 10 days, inoculated plantlets had a significant increase in height (54.5%), root fresh matter
121 (88.6%), root dry matter (61.4%), shoot fresh matter (13.8%) and root length (40%). No
122 significant difference was found for shoot dry matter (Figure S2).
123 Under gnotobiotic conditions, inoculated plantlets showed a larger diazotrophic
124 bacteria population associated with rhizosphere, rhizoplane, and roots (Figure S3). For
125 rhizosphere and rhizoplane compartments, the population density was significantly greater than
126 control plantlets (approximately 1.5 $\log_{10}$ bacteria cell per g of soil or root). The bacterial
127 population inside the plantlets showed no difference between inoculated and non-inoculated
128 plantlets, further supporting that *Azospirillum* sp. UENF-412522 preferentially colonizes the
129 rhizosphere/rhizoplane. In parallel, samples from seedlings inoculated with *Azospirillum* sp.
130 UENF-412522 at 1 and 7 days after germination (d.a.g.) were viewed under SEM (Figure 2),
131 confirming the root surface as the preferential colonization site. After radicle emergence, single
132 cells were noted at the bottom region of the radicle (Figure 2A), and bacteria aggregates can be
133 seen in the vicinity of the crack zone between the radicle and the tegument (Figure 2C-D).
134 Interestingly, sparse stomata-like structures were seen at the radicle, which seems to be an

135 infection point for the bacteria (Figure 2B). Bacteria cells interact with the root surface mainly
136 by apolar attachment and by fibrillar material anchoring the plant cell-wall, establishing an
137 aggregate network (Figure 2E). At seven d.a.g., bacteria successfully colonized the root hair zone
138 (Figure 2F) and the elongation/differentiation zone (Figure 2G) of the main developed root.
139
140 **Genome assembly and strain identification**
141 The promising *in vitro* and *ex vitro* results prompted us to sequence the *Azospirillum sp.* UENF-
142 412522 genome. We used an Illumina HiSeq 2500 instrument (paired-end mode, 2 × 100 bp
143 reads). Sequencing reads were quality filtered and assembled with SPAdes (see methods for
144 details). The assembly consists of 101 contigs (length ≥ 500 bp), encompassing 7,360,543 bp,
145 with a 67.92% GC content, N50 and L50 of 175,376 bp and 13 respectively. The genome harbors
146 6,508, 71 and 8 protein-coding, tRNA and rRNA genes, respectively.
147 Genome relatedness within the *Azospirillum* genus was computed using the average
148 nucleotide identity (ANI) and digital DNA-DNA hybridization (dDDH) of all *Azospirillum* spp.
149 genomes deposited in RefSeq (n = 48). ANI values were used to build a genome-to-genome
150 distance matrix and a neighbor-joining dendrogram (Figure 3A). This analysis clearly shows
151 distinct clusters comprising *A. brasilense* and *A. tiophilum* isolates. In contrast, none of the
152 remaining strains formed a consistent clade. Further, *A. lipoferum* RC and 4B isolates did not
153 cluster together, indicating that they do not belong to the same species. We found greater
154 genetic diversity in the isolates that do not belong to these clusters (Figure 3B). Among those is
155 *Azospirillum* sp. UENF-412522, which does not cluster with any other known strain, suggesting
156 that it represents a novel *Azospirillum* species.
157 Even though the *Azospirillum* genus has more than 15 described species, genomic data
158 are biased towards *A. brasilense*, which accounts for 37% (19 isolates) of the available genomes
159 (Figure 3). We also noticed that five isolates have similar names and share more than 99.9% and
160 70% in ANI and dDDH analyses, respectively. We removed these redundant genomes from the
161 downstream analyses and used GCF_001315015, GCF_003119195, GCF_003119115, and
162 GCF_004923295 as representatives of *A. brasilense* Sp7, *A. brasilense* Sp245, *Azospirillum* sp.
163 TSH58 and *Azospirillum* sp. TSH100 respectively. Hence, the dataset used in the next sections
164 comprises 43 publicly available genomes and that of *Azospirillum* sp. UENF-412522 genome.
165
166 **Pangenome analyses of the *Azospirillum* genus**
167 The pangenome is the complete gene repertoire of a given clade (e.g., a species) [28]. We
168 employed a minimum identity threshold of 50% for gene family identification in *Azospirillum*.
169 The pangenome comprises 42,515 genes, including a core genome (i.e. genes present in all
170 isolates) of only 771 genes, likely because of the high diversity, prevalence of genomic
171 rearrangements, and low synteny of this genus [9]. We clustered the isolates based on their
172 gene presence/absence patterns and confirmed the high genomic heterogeneity across the
173 genus (Figure 4A). Our results also support an open pangenome, as it grows with the addition of
174 new genomes (Figure 4B). Similar results were previously shown in *Alphaproteobacteria* [29],
175 who found 220 core genes across 27 in *Novosphingobium* spp. genomes. The *Azospirillum* core
176 genome reported here is substantially greater than that, which could be at least partially
177 explained by the fact that the vast majority of the isolates studied here were obtained from soil
178 and plant tissues. *Azospirillum* sp. RU37 (GCF_900188305) and *Azospirillum* sp. RU38E
179 (GCF_900188385) share the majority of accessory clusters. The same pattern is observed for

180 *Azospirillum* sp. TSH20 (GCF_003115935) and *Azospirillum* sp. TSH7 (GCF_003115945). In both
181 cases, the genomes with unusually high accessory genome similarity also exhibit 100% of ANI
182 and dDDH, indicating that they belong to the same strain.
183 Next, we analyzed the unique gene complement of *Azospirillum* sp. UENF-412522. Out
184 of the 18,065 unique genes inferred by Roary, 405 belonged to this strain. Among these genes,
185 we identified creatinine amidohydrolase *crnA* (EI613_12750), an enzyme involved in the
186 degradation of creatinine [30], which has been reported as replication-impairing molecule in
187 bacteria [31]. The gene 3-alpha-hydroxysteroid dehydrogenase *hsdA* (EI613_09215), involved in
188 steroid catabolism, is also exclusive to this strain and might assist *Azospirillum* sp. UENF-412522
189 to use steroids as a carbon source [32]. We also found the two component system *prsDE*
190 (EI613_31600-31605) as exclusive to this strain. PrsDE produces a low molecular weight
191 succinoglycan, which might assist in plant colonization by *Azospirillum sp.* UENF-412522 [33].
192
193 **Plant growth promotion genes**
194 Plant growth modulation by bacteria is a complex process [34]. Several bacterial genes are often
195 associated with direct beneficial effects, such as those responsible for biological nitrogen
196 fixation (BFN), root growth enhancement, phosphate solubilization, and deviation of the
197 ethylene biosynthesis pathway towards ammonia and α-ketobutyrate. We assessed the
198 presence of genes that are likely involved in direct plant growth promotion across *Azospirillum*
199 strains, with a particular focus in *Azospirillum sp.* UENF-412522. This procedure was guided by a
200 maximum likelihood phylogenetic tree built with the protein sequences encoded by the core-
201 genome, which was combined with a gene presence/absence matrix (Figure 5). Below we
202 discuss these genes in light of the mechanisms by which they promote plant growth.
203 BNF is a major plant growth promotion mechanism present in several *Azospirillum*
204 strains [8, 35]. This process relies on the nitrogenase enzyme complex, which reduces
205 atmospheric nitrogen ($N_2$) to ammonium ($NH_4$). The *nifHDK* genes encode, respectively, a
206 nitrogenase iron (Fe) protein, a nitrogenase molybdenum-iron (MoFe) protein alpha chain, and
207 a nitrogenase MoFe protein beta chain. The FeMo co-factor (FeMoCo) present in the MoFe
208 protein binds $N_2$, while the Fe protein uses the energy from ATP hydrolysis to drive the reduction
209 of $N_2$ to $NH_4$ by FeMoCo [36]. We used the presence of the *nifHDK* genes to predict the nitrogen
210 fixation capacity across *Azospirillum* genomes. All the analyzed genomes have these genes,
211 except for *Azospirillum* sp. RU37A, *Azospirillum* sp. RU38E and *Azospirillum* sp. L-25-5w-1 (Figure
212 5). *Azospirillum* sp. UENF-412522 possesses the *nifHDK* (EI613_05225-05215) operon and a
213 *nifDK* (EI613_05195-05200) operon, resembling the distribution found in most of the other
214 *Azospirillum* genomes containing *nifHDK*. Some exceptions to this structure are found in *A.*
215 *brasilense* Sp245, which possesses four *nifDK*, including vanadium nitrogenase variants [37];
216 *Azospirillum* sp. B506 presents a single *nifK*, and; *Azospirillum* sp. RU37A and *Azospirillum* sp.
217 RU38E have two *nifD*. The presence of more than one *nifHDK* increase nitrogen fixation to the
218 bacteria and associated plants. However, given that BNF is energetically expensive, the selective
219 advantage of such increased activity remains unclear.
220 Most of the soil phosphate is insoluble and hence unavailable to direct plant
221 absorption [38]. Several PGPRs promote plant growth by releasing organic acids that chelate
222 divalent cations (e.g., $Ca^{2+}$) in poorly soluble mineral forms (e.g., hydroxyapatite), increasing P
223 availability [39]. Gluconic acid secretion is the best-characterized mechanism of phosphate
224 solubilization, that is performed by pyrroloquinoline quinone (PQQ)-dependent glucose

225 dehydrogenase (GDH) [40]. We used the presence of the genes encoding the PQQ co-factor as
226 a proxy to understand P solubilization through GDH-PQQ in *Azospirillum* spp. The *pqq* genes
227 found in *Azospirillum* sp. were *pqqABCDE* (EI613_19670-19690). While *Azospirillum* UENF-
228 412522 and *A. halopraeferens* DSM3675 harbor the complete operon, all other strains lack *pqqA*
229 (Figure 5). The *pqq* operon is absent in three strains (*Azospirillum* sp. RU37A, *Azospirillum* sp.
230 RU38E, *Azospirillum* sp. L-25-5w-1). *A. brasilense* FP2 lacks *pqqA* and *pqqD*. Interestingly,
231 phytase genes were only found in the pqq-lacking strains *Azospirillum* sp. RU37A and
232 *Azospirillum* sp. RU38E, indicating that the capacity to mobilize P from organic compounds
233 displaced PQQ-dependent P solubilization in these bacteria.
234 Although *pqqA* has been regarded as non-essential for PQQ biosynthesis [41], other
235 studies support its role as the backbone for PQQ biogenesis [42]. PqqA binds to PqqD, prior to
236 PqqAD interaction with PqqE [43]. The crucial role of *pqqA* and *pqqB* was also confirmed by
237 knockout mutants of *Rahnella aquatilis* HX2, which showed decreased biocontrol and mineral P
238 solubilization [44]. A direct correlation between *pqqB* and *pqqF* expression and PQQ production
239 has also been shown [45]. Further, the same authors also reported that *Pseudomonas putida*
240 KT2440 *pqqF* is controlled by an independent promoter and terminator, allowing this gene to
241 modulate PQQ levels [45]. The presence of incomplete *pqq* operons in many *Azospirillum* strains
242 allows one to speculate that these isolates have other genes to compensate for the absence of
243 *pqqA*, a hypothesis that warrants experimental validation. Further, upstream of *pqqABCDE*, we
244 found an alcohol dehydrogenase ADH IIB *qbdA* (EI613_19655) and its associated regulator *amgR*
245 (EI613_19660), which are possibly related to acetic acid production mediated by PQQ [46]. This
246 operon also has a a gene encoding a hypothetical protein containing a CXXCW motif, present in
247 several soil bacteria, which might be associated with PQQ catabolism (TIGR03865). Hence, the
248 *pqqABCDE* operon might be co-regulated with *qdbA* in *Azospirillum* sp. UENF-412522.
249 Ethylene is a plant hormone with a central role in senescence and growth of leaves,
250 flowers, and fruits [47]. Under stress conditions, ethylene can impair plant cell elongation [48].
251 Ethylene is synthesized by the oxidation of 1-aminocyclopropane-1-carboxylate (ACC) by ACC
252 oxidase. ACC can be broken down into α-ketobutyrate and $NH_3$ by ACC deaminase [49], an
253 enzyme produced by several PGPR that induce plant growth by lowering ethylene levels under
254 stress conditions. We identified the ACC deaminase gene (*acdS*, EI613_03680) in *Azospirillum*
255 sp. UENF-412522 and other 11 *Azospirillum* sp. strains, supporting that their association with
256 plants can alleviate ethylene-mediated growth inhibition. Importantly, we have not found *acdS*
257 in *A. brasilense* strains.
258 Considering its gene complement, *Azospirillum sp.* UENF-412522 has a significant
259 potential to promote root growth. Despite the strong experimental evidence supporting IAA
260 biosynthesis, we found none of the classic auxin biosynthesis genes (i.e., *ipdC*, *iaaH* and *iaaM*)
261 [50-52], which prompted us to investigate other IAA biosynthesis pathways [51] in this strain.
262 Interestingly, we found a gene encoding a nitrilase (*nit*, EI613_03300), which is 74% similar that
263 encoded by a *nit* that converts indole-3-acetonitrile (IAN) directly into IAA or into indol-3-
264 acetamide (IAM) in the rhizobacterium *Pseudomonas* sp. UW4 [53, 54]. In the latter pathway,
265 the conversion of IAM into IAA requires the action of IAM-hydrolases, for which we found two
266 candidate genes, EI613_04545 e EI613_07015. These genesare similar to amide hydrolases from
267 *Rhodococcus* sp. (Q53116) [55, 56] and *Agrobacterium fabacearum* (ADY67766.1) [57],
268 respectively. The apparent absence of tryptophan monooxygenase genes, which catalyze the
269 conversion of Trp into IAM, indicates that *Azospirillum* sp. UENF 412522 produces IAA through

270 an interplay between the IAN and IAM pathways, as reported in *Rhizobium* spp. and
271 *Bradyrhizobium* spp. [53, 58]. Nevertheless, the initial steps in the production of IAN in
272 *Azospirillum* sp. UENF 412522 are yet to be elucidated. In contrast, all *A. brasilense* strains
273 possess the gene *ipdC* (Figure 5), supporting the ability of this species to synthesize IAA by the
274 indole-3-pyruvate pathway, as experimentally demonstrated [59, 60]. Another eight *A.*
275 *brasilense* strains possess nitrile hydratase (*nthB*) and *iaaH* genes, which contribute to IAA
276 production by the conversion of IAN to IAM, and from IAM to IAA, respectively.
277 We also investigated *Azospirillum sp.* UENF-412522 genes that might promote root
278 development through the emission of nitrite and nitric oxide. *A. brasilense* is known for secreting
279 nitrite as a product of nitrate respiration [61, 62]. *Azospirillum sp.* UENF-412522 has a nitrate
280 reductase operon *napCAB* (EI613_10540-10550). *napA* encodes a periplasmic nitrate reductase,
281 while *napCB* encodes electron transfer subunits necessary for napA activity. This operon was
282 proposed as an alternative electron acceptor for oxygen in *A. brasilense* sp. 245 periplasm [63]
283 and is possibly responsible for nitrate respiration in *Azospirillum sp.* UENF-412522. The nitrite
284 generated by nitrate respiration can be exported to the environment, absorbed by the plant
285 root, and reduced to nitric oxide. Under acidic pH, nitrite can be reduced to nitric oxide without
286 enzymatic action [64] and absorbed by root cells [65]. The downside of nitrate respiration to
287 plant growth promotion is the reduction of available nitrogen in the system and the production
288 of greenhouse gases. Hence, we hypothesize that *Azospirillum* sp. UENF-412522 nitrogen
289 fixation contributes to nitrate respiration and plant absortion.
290 Most known *Azospirillum* strains are diazotrophs. $N_2$-fixation requires a microaerophilic
291 or anoxic environment because nitrogenase metalloclusters are sensitive to oxygen. Previous
292 works in *Azospirillum* proposed that complete oxygen depletion inhibited nitrogenase activity
293 [66], while others suggest otherwise [67]. *Azospirillum sp.* UENF-412522 was isolated from the
294 rhizoplane, where low oxygen conditions are rather common [68]. Given the genomic
295 investigations reported here, we hypothesize that P solubilization, root growth enhancement by
296 nitrate respiration, and $N_2$ fixation are dependent of an anoxic environment and might be
297 interconnected in the soil-root system (Figure 6). Under low oxygen availability, nitrate is used
298 as final electron acceptor in anaerobic respiration, producing nitrite, which is reduced to nitric
299 oxide under low pH in the periplasm. Such acidic environment can be harnessed by the gluconic
300 acid generated by the PQQ-dependent glucose dehydrogenase. Nitric oxide or nitrite would then
301 be exported to the rhizosphere, stimulating root growth. Finally, gluconic acid is also exported
302 to the rhizosphere, solubilizing phosphate for the root cells uptake.
303
304 **Antibiotic resistance genes**
305 *Azospirillum sp.* UENF-412522 has several antibiotic resistance genes, such as those conferring
306 resistance to: fosmidomycin (*fsr*, EI613_04505) [69], bicyclomycin (*bcr*, EI613_29470,
307 EI613_14405) [70], bacitracin (*uppP/BacA*, EI613_27660) [71], tabtoxin (*ttr*, EI613_22745) [72],
308 phenazine (*ehpR*, EI613_22490) [73], and tetracycline (*tetA*, EI613_26440) [74]. We also found
309 multiple drug resistance genes (*mdtABCE*, EI613_19480-19470) [75], *acrAB* (EI613_25875-
310 25880) [76], and *norM* (EI613_15640) [77]. Interestingly, most of these antibiotics, such as
311 bicyclomycin [78], phenazine [79], bacitracin, and tetracycline [80], are commonly produced
312 *Streptomyces*, which is abundant in the soil, where it plays a key role in plant organic matter
313 decomposition [81, 82]. The presence of genes conferring resistance against *Streptomyces*

314 antimicrobials is likely important to the survival of *Azospirillum sp.* UENF-412522 in the
315 rhizosphere.
316
317 **CONCLUSION**
318 In the present study we described *Azospirillum sp.* UENF-412522, a new *Azospirillum* plant
319 growth-promoting species. We experimentally demonstrated that this bacterium is able to fix
320 nitrogen, produce IAA, solubilize mineral P, and recognize and colonize seed-root surfaces. This
321 strain is equipped with genes involved in BNF, P solubilization, ethylene catabolism, promotion
322 of root development, and antibiotic resistance in the rhizosphere. Collectively, our results
323 support the biotechnological potential of *Azospirillum sp.* UENF-412522 to be part of
324 bioinoculant formulations for sustainable agriculture. We also propose a system involved in the
325 partitioning of the fixed nitrogen between nitrate respiration and plant absorption, which is
326 likely critical in plant-growth promotion under microaerophilic or anoxic conditions. Finally, this
327 study emphasizes the importance of comprehensive studies using genomic, microscopy,
328 microbiological, and biochemical approaches to characterize novel *Azospirillum* species outside
329 of the *A. brasilense* clade, which could unlock the genus diversity and open novel possibilities
330 for agricultural applications.
331
332 **METHODS**
333 **Bacterial isolation and DNA purification**
334 Passion fruit (*Passiflora edulis* f. *edulis*) root samples were obtained at the Integrated
335 Agroecological Production System (SIPA), Embrapa Agrobiologia, Seropédica, Rio de Janeiro,
336 Brazil (coordinates 22.7635°S 43.6886°W) and taken to the laboratory in a sterilized plastic bag
337 kept in ice. Rhizoplane bacteria isolation was performed by an adapted version of Bramwell et
338 al. (1995)[83]. In summary, root axis segments (10 g fresh weight) were sealed from both tip
339 sides with paraffin, gently washed in tap water, and transferred to a 250 mL glass flask
340 containing 90 mL of saline solution (NaCl, 0.9%). Roots were kept under agitation for 5 min at a
341 rotatory shaker (200 rpm at 30 °C) to remove soil particles. After that, the same sealed root
342 segment was carefully transferred to another 250 mL glass flask containing 90 mL of sterile saline
343 (NaCl, 0.9%) solution plus 10 g of autoclaved sieved sand, where remained under agitation for
344 10 min at rotatory shaker (150 rpm at 30 °C) to detach bacteria cells from root surfaces
345 (rhizoplane bacteria fraction). After sand decantation, 10 mL of the suspension were transferred
346 to 90 mL of sterile saline solution ($10^{-1}$ dilution), which were used to prepare successive dilutions
347 until $10^{-6}$. Three independent 20 µL aliquots of all serial dilutions ($10^{-2}$ to $10^{-6}$) were inoculated
348 into glass vials (16 mL volume) containing 5 mL NFb nitrogen-free semisolid medium
349 (composition in g $L^{-1}$): malic acid, 5.0; $K_2HPO_4$, 0.5; $MgSO_4.7H_2O$, 0.2; NaCl, 0.1; $CaCl_2$. $2H_2O$, 0.02;
350 micronutrient stock solution ($CuSO_4.5H_2O$, 0.04; $ZnSO_4.7H_2O$, 0.12; $H_3BO_3$, 1.40; $Na_2MoO_4.2H_2O$,
351 1.0; $MnSO_4$. $H_2O$, 1.175. Complete volume to 1,000 mL with distilled water), 2 mL; bromothymol
352 blue (5 g $L^{-1}$ in 0.2 N KOH), 2 mL; FeEDTA (solution 16.4 g $L^{-1}$), 4 mL; vitamin stock solution
353 (biotin, 10 mg; pyridoxal-HCl, 20 mg in 100 mL distilled water), 1 mL; KOH, 4.5 g; distilled water
354 to bring the final volume to 1,000 mL and adjust pH to 6.5. A quantity of 1.6 g agar $L^{-1}$ was added
355 to prepare the semisolid medium [84].
356 Inoculated NFb vials were incubated in a growth chamber at 30 °C for 5 to 7 days. The
357 growth of diazotrophic bacteria was characterized by the formation of a subsurface white
358 pellicle. Using a loopful, a sample of the pellicle from the last positive dilution was inoculated in

359 a fresh NFb N-free semisolid medium and incubated under the same conditions described
360 above. This process was subsequently conducted for three times and the last new pellicle
361 formed was streaked onto DYGS solid medium plates for colony purification. The DYGS
362 composition (g $L^{-1}$): glucose, 2.0; malic acid 2.0; peptone, 1.5; yeast extract, 2.0; $K_2HPO_4$, 0,5;
363 $MgSO_4.7H_2O$, 0.5; glutamic acid, 1.5, pH is 6.5. The purified isolate was stored in 10% glycerol at
364 -80 ºC, under the code UENF-412522, as a diazotrophic bacterium associated with the passion
365 fruit rhizoplane.
366 For DNA extraction, 100 µL of the stored bacteria were transferred to a glass tube
367 containing 5 mL DYGS liquid medium and grown in an orbital shaker at 30 °C and 180 rpm for 48
368 hours. After that, 20 µL were transferred to the same medium and grown at the same conditions
369 for 24 h. An aliquot of 200 µL was taken, and bacterial genomic DNA was extracted using the
370 QIAamp kit (QIAGEN) following the manufacturer's instructions. DNA was quantified in a 3000
371 NanoDrop (Thermo Scientific USA). DNA quality was analyzed using a 0.8% agarose gel stained
372 with gel red.
373 To obtain an initial taxonomic assignment, PCR was conducted with the primers 27F (5`-
374 AGAGTTTGATCMTGGCTCAG 3`) and 1492R (5'-TACGGYTACCTTGTTACGACTT-3`). These
375 reactions were performed using 50 ng of genomic DNA in 25 µL final reaction volume,
376 containing: 2 µL of dNTPs (20 mM each) 2.5 µL of 10 x enzyme buffer, 0.75 µL 50 mM $MgCl_2$, 2.5
377 µL of each primer (5 mM), 0.3 µL Taq polymerase (5 U/µL). Amplification was performed in a 96-
378 well thermocycler Veriti model (Applied Biosystems), programmed at 9°C for 3 min, 30 cycles of
379 amplification (94°C for 1 min, 55 °C for 30 s, 72 °C for 30 s) at 72 °C for 10 min. The sequencing
380 reactions were performed using the Big Dye Terminator Sequencing Kit-Cycle Sequencing Ready
381 ABI Prism version 3 (Life Technologies, USA), following manufacturer's recommendations.
382 Sequencing was performed on ABI Sequencer model 3130 (Applied Biosystems).
383
384 **Plant growth promotion traits of UENF-412522 bacterial strain**
385 ***nifH gene detection***
386 The *nifH* presence were assessed by PCR, with the primers PolF (5'TGCGAYCCSAARGCBGACTC
387 3`) and PolR (5'ATSGCCATCATYTCRGCCGA 3') [85]. In each reaction, we used 1 µL dNTPs (200
388 mM each), 5 µL of 10X buffer, 4 µL of 25 mM $MgCl_2$, 0.5 µL of each primer (10 mM), 0.25 µL Taq
389 polymerase (5 U/ µL) and 50 ng DNA, in a final volume of 50 µL. The amplification conditions
390 were denaturation at 94 °C for 5 minutes, then 30 cycles (94 °C for 1 min, 55 ºC for 1 min, 72 °C
391 for 2 minutes) and a final extension step (72 °C for 5 min). PCR products were inspected on 1.5%
392 agarose gels. Bp-100 DNA ladder (Invitrogen) was used as a molecular weight marker.
393
394 ***Acetylene reduction activity assay (ARA)***
395 The *in vitro* nitrogen fixation ability of UENF-412522 was evaluated using the acetylene
396 reduction assay (ARA), as previously described by Baldani [84]. The strain was grown in 16 mL
397 glass vials containing 5 mL of N-free NFB semisolid medium, as described above. These flasks
398 were inoculated with 20 µL of the bacterial inoculum suspended in sterile water, adjusted to an
399 optical density (OD) of 1.0, and incubated at 30 °C for 48 h. After pellicle formation, the vials
400 were closed with a sterilized pierceable rubber stopper of the subseal type. Syringes were used
401 to remove 1 mL of air and to inject 1 mL of acetylene in each vial. The flasks were incubated at
402 30 °C for 1 h, and 1 mL of the gas phase was analyzed on a gas chromatograph with flame
403 ionization (Perkin Elmer), to determine the ethylene concentration in the sample.

404 ***Phosphorus and zinc solubilization***
405 Phosphate solubilization was independently carried out using 1 $g.L^{-1}$ Araxá rock phosphate
406 [$Ca_{10}(PO_4)_6F_2$] and tricalcium phosphate [$Ca_3(PO_4)_2$]. Bacterial cultures grown in DYGS liquid
407 medium adjusted to an optical density of 1.0 were inoculated (20 µL) at the center of the petri
408 dish with agar containing Pikovskaya medium. After this procedure, they were incubated at 30
409 °C for 7 days. The ability of the isolates in solubilizing P was evaluated by measuring the
410 translucent halo, according to Kumar and Narula formula [86], in which S.I. (solubility index) =
411 halo Diameter (mm)/colony diameter (mm). We conducted three biological replicates of this
412 assay.
413 We also assessed P solubilization in Pikovskaya liquid medium supplemented with $1g.L^{-}$
414 $^{1}$ of the Araxá rock phosphate or $Ca_{10}(PO_4)_6F_2$ was used to quantify the soluble P. Aliquots of 100
415 µL of bacterial cultures grown in DYGS liquid medium were transferred to 50 mL tubes containing
416 Pikovskaya medium and kept for 7 days under constant agitation at 150 rpm in a rotatory shaker
417 at 30 °C. After this period, cultures were centrifuged at 3200 rpm for 15 minutes, and the
418 supernatant was used for pH determination and quantification of soluble P.
419 Zinc solubilization was carried out according to Intorne et al [87]. Aliquots of 20 µL of
420 bacterial strains cultivated for 24 h at 30 °C in DYGS liquid medium, adjusted to an optical density
421 of 1.0, were inoculated at the center of the petri dish containing Saravanan medium with agar
422 supplemented with $1g.L^{-1}$ of ZnO and incubated at 30 °C for 7 days. After this period, the ability
423 to solubilize ZnO was also performed according to Kumar and Narula [86]. We conducted three
424 biological replicates of this assay.
425
426 ***Indole acetic acid (IAA) production***
427 Bacterial isolates were cultured in liquid DYGS medium for 24 h at 30 °C and transferred (25 µL)
428 to test tubes containing 5 mL of the same medium in the presence and absence of L-tryptophan
429 (100 $mg.L^{-1}$) before incubation in the dark for 72 h at 30 °C, shaking at 150 rpm. The cultures
430 were then transferred to 2 mL tubes and centrifuged at 10,000 rpm for 10 min, and the
431 supernatant transferred to a test tube with 2 mL of Salkowski reagent [88]. Tubes were
432 incubated for 30 min in the dark. The production of IAA was evaluated by the presence of pink
433 color in the tubes, and the color intensity was determined with a spectrophotometer at a
434 wavelength of 530 nm. IAA concentrations were measured using a calibration curve.
435
436 ***Biochemical API 50 CH/E test***
437 For the metabolic characterization of bacterial isolates, we used the API 50 CH/E test kit
438 (bioMérieux SA Marcy- l'Etoile/France), which evaluates the ability of the isolates to conduct
439 fermentation of 49 carbohydrates and derivatives. To this end, the isolates were cultured in
440 DYGS medium for 24 h at 150 rpm. After this period, the isolates were suspended in autoclaved
441 water and adjusted to optical density 1.0; 2 mL of this suspension were added to the CHL
442 medium (bioMérieux) and transferred to galleries containing different substrates. Each dome
443 was sealed with a sterile drop of mineral oil and incubated in an environmental chamber at 37
444 °C. Reads were recorded after 24 h and 48 h after inoculation, and eventual production of
445 organic acids during incubation shifts the pH indicator from red to yellow.
446
447 **Plant growth promotion assay under greenhouse conditions**

448 A greenhouse assay was carried out to evaluate the effect of UENF-412522 inoculation in plants.
449 To perform it, passion fruit seeds of the cultivar Yellow master FB200 were disinfected in 1%
450 sodium hypochlorite solution for 20 minutes, followed by three rinses in autoclaved distilled
451 water and then transferred to germitest paper moistened with autoclaved water. Then, the
452 seeds were incubated in a growth chamber at 30 °C, for 16 h in the light and 8 h in the dark.
453 After germinating, these seeds were transferred to styrofoam trays containing autoclaved plant
454 substrate under greenhouse conditions. After 30 days of transplanting, seedlings of
455 approximately 6 cm were transferred to a 300 mL plastic bag containing the same autoclaved
456 plant growth substrate. The inoculum of the UENF-412522 strain was prepared in liquid DYGS
457 medium after 40 h of growth in a rotatory shaker at 30 °C and 150 rpm. Bacterial suspensions
458 containing approximately $10^8$ cells.$mL^{-1}$ (O.D. = 1.0 at 600 ηm) were inoculated on the region of
459 the plant's neck, and plants were transferred to the greenhouse for 30 days. The assay was set
460 up in a randomized block design, two treatments (inoculated and non-inoculated plantlets) and
461 six replications. The control plants received 1 mL of the liquid DYGS medium containing lysed
462 UENF-412522 cells.
463
464 **Plant root colonization assay**
465 We evaluated plant-bacteria interaction by determining the population size and root
466 colonization by scanning electron microscopy (SEM). For this, passion fruit seeds of the Yellow
467 cultivar master FB200 were disinfected and placed to germinate as described above. After
468 germination, the seedlings were transferred to a test tube containing autoclaved vermiculite.
469 Then, 1 ml of bacterial suspension containing approximately $10^8$ cells $mL^{-1}$ was inoculated on the
470 seedling neck. Seedlings were kept for seven days after inoculation (d.a.i) in a culture room
471 under a temperature of 30ºC (16 h in the light and 8 hours in the dark). For SEM, root samples
472 were collected at 1 and 7 days after the inoculation of the bacterial suspension. Samples for SEM
473 were prepared according to Baldotto et al. [89] and viewed at Zeiss DSEM 962 at 15 Kv voltage
474 in secondary electron detector mode. The bacteria count at rhizosphere, rhizoplane, and roots
475 was performed at seven d.a.i., as described above. The control consisted of seedlings inoculated
476 with the DYGS medium.
477
478 **Genome sequencing and assembly**
479 The sequencing procedures and basic data processing were performed, as previously described
480 [25]. In summary, paired-end libraries were prepared using the TruSeq Nano DNA LT Library Prep
481 (Illumina) and sequenced on a HiSeq 2500 instrument at the Life Sciences Core Facility (LaCTAD;
482 UNICAMP, Campinas, Brazil). Sequencing reads (2 × 100 bp) had their quality checked with
483 FastQC 0.11.5 (https://www.bioinformatics.babraham.ac.uk/projects/fastqc/). Quality filtering
484 was performed with Trimmomatic 0.35 [90], and reads with average quality below 30 were
485 discarded. The genome assembly was performed using SPAdes 3.8 [91] and assembly metrics
486 evaluated by QUAST 3.0 [92].
487
488 **Genome annotation and phylogenetic analysis**
489 The assembled genome was annotated with the NCBI Prokaryotic Genome Annotation Pipeline
490 [93]. The *Azospirillum* sp. UENF-412522 genome was deposited on Genbank under the
491 BioProject PRJNA508400. *Azospirillum* spp. genomes available in RefSeq [94, 95] were
492 downloaded (n = 48, as of June 03 2019) and protein sequences were predicted using PROKKA

1.13.3 [96]. We searched for proteins encoded by genes potentially involved in plant growth promotion using a blastp [97] search on the SwissProt database, with minimum coverage and similarity thresholds of 70% and 60%, respectively. All-against-all average nucleotide identity (ANI) was computed using pyani 0.28 [98]. Pan-genome analysis was performed with Roary 3.12.0, with a minimum identity threshold of 50% [99]. Multiple sequence alignments were performed using Muscle 3.8.30 [100] and phylogenetic reconstructions performed with RAxML 8.2.10 [101].

## AUTHOR CONTRIBUTIONS

Conceived the study: FLO, TMV; Funding and resources: FLO, TMV; Data analysis: GLR, FPM, RKG, FP-S, DC-A, IP-O; Performed experiments: PSLG, STS, AFA; Interpretation of the results: GLR, FPM, FLO, TMV; Wrote the manuscript: GLR, FPM, FLO, TMV.

## ACKNOWLEDGEMENTS

This work was supported by Fundação Carlos Chagas Filho de Amparo à Pesquisa do Estado do Rio de Janeiro (FAPERJ; grants E-26/111.827/2013, E-26/102.259/2013, E-26/201.239/2014, E-26/203.309/2016 and E-26/203.014/2018), Coordenação de Aperfeiçoamento de Pessoal de Nível Superior - Brasil (CAPES; Finance Code 001), and Conselho Nacional de Desenvolvimento Científico e Tecnológico (CNPq; grant 449904/2014-8 and 314263/2018-7). The funding agencies had no role in the design of the study and collection, analysis, and interpretation of data and in writing.

## REFERENCES

1. Bourguet D, Guillemaud T: **The hidden and external costs of pesticide use**. In: *Sustainable Agriculture Reviews.* Springer; 2016: 35-120.
2. Maroniche GA, Diaz PR, Borrajo MP, Valverde CF, Creus CM: **Friends or foes in the rhizosphere: traits of fluorescent Pseudomonas that hinder Azospirillum brasilense growth and root colonization**. *FEMS Microbiol Ecol* 2018, **94**(12).
3. Vejan P, Abdullah R, Khadiran T, Ismail S, Nasrulhaq Boyce A: **Role of Plant Growth Promoting Rhizobacteria in Agricultural Sustainability-A Review**. *Molecules* 2016, **21**(5).
4. Prasad M, Srinivasan R, Chaudhary M, Choudhary M, Jat LK: **Plant Growth Promoting Rhizobacteria (PGPR) for Sustainable Agriculture: Perspectives and Challenges**. In: *PGPR Amelioration in Sustainable Agriculture.* Elsevier; 2019: 129-157.
5. Brink SC: **Unlocking the Secrets of the Rhizosphere**. *Trends Plant Sci* 2016, **21**(3):169-170.
6. Ahkami AH, White III RA, Handakumbura PP, Jansson C: **Rhizosphere engineering: Enhancing sustainable plant ecosystem productivity**. *Rhizosphere* 2017, **3**:233-243.
7. Mehnaz S: **Azospirillum: a biofertilizer for every crop**. In: *Plant Microbes Symbiosis: Applied Facets.* Springer; 2015: 297-314.
8. Fukami J, Cerezini P, Hungria M: **Azospirillum: benefits that go far beyond biological nitrogen fixation**. *AMB Express* 2018, **8**(1):73.
9. Wisniewski-Dye F, Borziak K, Khalsa-Moyers G, Alexandre G, Sukharnikov LO, Wuichet K, Hurst GB, McDonald WH, Robertson JS, Barbe V *et al*: **Azospirillum genomes reveal**

537 **transition of bacteria from aquatic to terrestrial environments**. *PLoS Genet* 2011,
538 **7**(12):e1002430.
539 10. Tarrand JJ, Krieg NR, Dobereiner J: **A taxonomic study of the Spirillum lipoferum**
540 **group, with descriptions of a new genus, Azospirillum gen. nov. and two species,**
541 **Azospirillum lipoferum (Beijerinck) comb. nov. and Azospirillum brasilense sp. nov**.
542 *Can J Microbiol* 1978, **24**(8):967-980.
543 11. Reis VM, Baldani VLD, Baldani JI: **Isolation, Identification and Biochemical**
544 **Characterization of Azospirillum spp. and Other Nitrogen-Fixing Bacteria**. In:
545 *Handbook for Azospirillum: Technical Issues and Protocols.* Edited by Cassán FD, Okon
546 Y, Creus CM. Cham: Springer International Publishing; 2015: 3-26.
547 12. Pankievicz VC, do Amaral FP, Santos KF, Agtuca B, Xu Y, Schueller MJ, Arisi AC, Steffens
548 MB, de Souza EM, Pedrosa FO *et al*: **Robust biological nitrogen fixation in a model**
549 **grass-bacterial association**. *Plant J* 2015, **81**(6):907-919.
550 13. Rodriguez H, Gonzalez T, Goire I, Bashan Y: **Gluconic acid production and phosphate**
551 **solubilization by the plant growth-promoting bacterium Azospirillum spp**.
552 *Naturwissenschaften* 2004, **91**(11):552-555.
553 14. Cohen AC, Bottini R, Pontin M, Berli FJ, Moreno D, Boccanlandro H, Travaglia CN,
554 Piccoli PN: **Azospirillum brasilense ameliorates the response of Arabidopsis thaliana**
555 **to drought mainly via enhancement of ABA levels**. *Physiol Plant* 2015, **153**(1):79-90.
556 15. Garcia JE, Maroniche G, Creus C, Suarez-Rodriguez R, Ramirez-Trujillo JA, Groppa MD:
557 **In vitro PGPR properties and osmotic tolerance of different Azospirillum native**
558 **strains and their effects on growth of maize under drought stress**. *Microbiol Res*
559 2017, **202**:21-29.
560 16. D'Angioli AM, Viani RAG, Lambers H, Sawaya ACHF, Oliveira RS: **Inoculation with**
561 **Azospirillum brasilense (Ab-V4, Ab-V5) increases Zea mays root carboxylate-**
562 **exudation rates, dependent on soil phosphorus supply**. *Plant and soil* 2017, **410**(1-
563 2):499-507.
564 17. Vacheron J, Renoud S, Muller D, Babalola OO, Prigent-Combaret C: **Alleviation of**
565 **abiotic and biotic stresses in plants by Azospirillum**. In: *Handbook for Azospirillum.*
566 Springer; 2015: 333-365.
567 18. Cassán F, Diaz-Zorita M: **Azospirillum sp. in current agriculture: From the laboratory**
568 **to the field**. *Soil Biology and Biochemistry* 2016, **103**:117-130.
569 19. Hungria M, Ribeiro RA, Nogueira MA: **Draft Genome Sequences of Azospirillum**
570 **brasilense Strains Ab-V5 and Ab-V6, Commercially Used in Inoculants for Grasses and**
571 **Legumes in Brazil**. *Genome Announc* 2018, **6**(20).
572 20. Blaha D, Prigent-Combaret C, Mirza MS, Moënne-Loccoz Y: **Phylogeny of the 1-**
573 **aminocyclopropane-1-carboxylic acid deaminase-encoding gene acdS in**
574 **phytobeneficial and pathogenic Proteobacteria and relation with strain**
575 **biogeography**. *FEMS Microbiology Ecology* 2006, **56**(3):455-470.
576 21. Esquivel-Cote R, Ramírez-Gama RM, Tsuzuki-Reyes G, Orozco-Segovia A, Huante PJP,
577 Soil: **Azospirillum lipoferum strain AZm5 containing 1-aminocyclopropane-1-**
578 **carboxylic acid deaminase improves early growth of tomato seedlings under nitrogen**
579 **deficiency**. 2010, **337**(1):65-75.

580 22. Vikram A, Alagawadi AR, Krishnaraj PU, Mahesh Kumar KSJWJoM, Biotechnology:
581 **Transconjugation studies in Azospirillum sp. negative to mineral phosphate**
582 **solubilization**. 2007, **23**(9):1333-1337.
583 23. Kaneko T, Minamisawa K, Isawa T, Nakatsukasa H, Mitsui H, Kawaharada Y, Nakamura
584 Y, Watanabe A, Kawashima K, Ono A *et al*: **Complete genomic structure of the**
585 **cultivated rice endophyte Azospirillum sp. B510**. *DNA Res* 2010, **17**(1):37-50.
586 24. Malhotra M, Srivastava S: **An ipdC gene knock-out of Azospirillum brasilense strain**
587 **SM and its implications on indole-3-acetic acid biosynthesis and plant growth**
588 **promotion**. *Antonie Van Leeuwenhoek* 2008, **93**(4):425-433.
589 25. Matteoli FP, Passarelli-Araujo H, Reis RJA, da Rocha LO, de Souza EM, Aravind L,
590 Olivares FL, Venancio TM: **Genome sequencing and assessment of plant growth-**
591 **promoting properties of a Serratia marcescens strain isolated from vermicompost**.
592 *BMC Genomics* 2018, **19**(1):750.
593 26. Matteoli FP, Passarelli-Araujo H, Pedrosa-Silva F, Olivares FL, Venancio TM: **Population**
594 **structure and pangenome analysis of Enterobacter bugandensis uncover the**
595 **presence of blaCTX-M-55, blaNDM-5 and blaIMI-1, along with sophisticated iron**
596 **acquisition strategies**. *Genomics* 2020, **112**(2):1182-1191.
597 27. Eckert B, Weber OB, Kirchhof G, Halbritter A, Stoffels M, Hartmann A: **Azospirillum**
598 **doebereinerae sp. nov., a nitrogen-fixing bacterium associated with the C4-grass**
599 **Miscanthus**. *Int J Syst Evol Microbiol* 2001, **51**(Pt 1):17-26.
600 28. Xiao J, Zhang Z, Wu J, Yu J: **A brief review of software tools for pangenomics**.
601 *Genomics Proteomics Bioinformatics* 2015, **13**(1):73-76.
602 29. Kumar R, Verma H, Haider S, Bajaj A, Sood U, Ponnusamy K, Nagar S, Shakarad MN,
603 Negi RK, Singh Y *et al*: **Comparative Genomic Analysis Reveals Habitat-Specific Genes**
604 **and Regulatory Hubs within the Genus Novosphingobium**. *mSystems* 2017, **2**(3).
605 30. Beuth B, Niefind K, Schomburg D: **Crystal structure of creatininase from Pseudomonas**
606 **putida: a novel fold and a case of convergent evolution**. *J Mol Biol* 2003, **332**(1):287-
607 301.
608 31. McDonald T, Drescher KM, Weber A, Tracy S: **Creatinine inhibits bacterial replication**.
609 *J Antibiot (Tokyo)* 2012, **65**(3):153-156.
610 32. Mobus E, Maser E: **Molecular cloning, overexpression, and characterization of**
611 **steroid-inducible 3alpha-hydroxysteroid dehydrogenase/carbonyl reductase from**
612 **Comamonas testosteroni. A novel member of the short-chain**
613 **dehydrogenase/reductase superfamily**. *J Biol Chem* 1998, **273**(47):30888-30896.
614 33. York GM, Walker GC: **The Rhizobium meliloti exoK gene and prsD/prsE/exsH genes**
615 **are components of independent degradative pathways which contribute to**
616 **production of low-molecular-weight succinoglycan**. *Mol Microbiol* 1997, **25**(1):117-
617 134.
618 34. Numan M, Bashir S, Khan Y, Mumtaz R, Shinwari ZK, Khan AL, Khan A, Al-Harrasi A:
619 **Plant growth promoting bacteria as an alternative strategy for salt tolerance in**
620 **plants: A review**. *Microbiol Res* 2018, **209**:21-32.
621 35. Steenhoudt O, Vanderleyden J: **Azospirillum, a free-living nitrogen-fixing bacterium**
622 **closely associated with grasses: genetic, biochemical and ecological aspects**. *FEMS*
623 *Microbiol Rev* 2000, **24**(4):487-506.

624 36. Dixon R, Kahn D: **Genetic regulation of biological nitrogen fixation**. *Nat Rev Microbiol*
625 2004, **2**(8):621-631.
626 37. Wisniewski-Dye F, Lozano L, Acosta-Cruz E, Borland S, Drogue B, Prigent-Combaret C,
627 Rouy Z, Barbe V, Herrera AM, Gonzalez V *et al*: **Genome Sequence of Azospirillum**
628 **brasilense CBG497 and Comparative Analyses of Azospirillum Core and Accessory**
629 **Genomes provide Insight into Niche Adaptation**. *Genes (Basel)* 2012, **3**(4):576-602.
630 38. Ewel JJ, Schreeg LA, Sinclair TR: **Resources for Crop Production: Accessing the**
631 **Unavailable**. *Trends Plant Sci* 2019, **24**(2):121-129.
632 39. Sharma SB, Sayyed RZ, Trivedi MH, Gobi TA: **Phosphate solubilizing microbes:**
633 **sustainable approach for managing phosphorus deficiency in agricultural soils**.
634 *Springerplus* 2013, **2**:587.
635 40. Alori ET, Glick BR, Babalola OO: **Microbial Phosphorus Solubilization and Its Potential**
636 **for Use in Sustainable Agriculture**. *Front Microbiol* 2017, **8**:971.
637 41. Toyama H, Lidstrom ME: **pqqA is not required for biosynthesis of pyrroloquinoline**
638 **quinone in Methylobacterium extorquens AM1**. *Microbiology* 1998, **144 ( Pt 1)**:183-
639 191.
640 42. Barr I, Latham JA, Iavarone AT, Chantarojsiri T, Hwang JD, Klinman JP: **Demonstration**
641 **That the Radical S-Adenosylmethionine (SAM) Enzyme PqqE Catalyzes de Novo**
642 **Carbon-Carbon Cross-linking within a Peptide Substrate PqqA in the Presence of the**
643 **Peptide Chaperone PqqD**. *J Biol Chem* 2016, **291**(17):8877-8884.
644 43. Latham JA, Iavarone AT, Barr I, Juthani PV, Klinman JP: **PqqD is a novel peptide**
645 **chaperone that forms a ternary complex with the radical S-adenosylmethionine**
646 **protein PqqE in the pyrroloquinoline quinone biosynthetic pathway**. *J Biol Chem*
647 2015, **290**(20):12908-12918.
648 44. Li L, Jiao Z, Hale L, Wu W, Guo Y: **Disruption of gene pqqA or pqqB reduces plant**
649 **growth promotion activity and biocontrol of crown gall disease by Rahnella aquatilis**
650 **HX2**. *PLoS One* 2014, **9**(12):e115010.
651 45. An R, Moe LA: **Regulation of Pyrroloquinoline Quinone-dependent glucose**
652 **dehydrogenase activity in the model rhizosphere-dwelling bacterium Pseudomonas**
653 **putida KT2440**. *Appl Environ Microbiol* 2016, **82**(16):4955-4964.
654 46. Yakushi T, Matsushita K: **Alcohol dehydrogenase of acetic acid bacteria: structure,**
655 **mode of action, and applications in biotechnology**. *Appl Microbiol Biotechnol* 2010,
656 **86**(5):1257-1265.
657 47. Iqbal N, Khan NA, Ferrante A, Trivellini A, Francini A, Khan MIR: **Ethylene Role in Plant**
658 **Growth, Development and Senescence: Interaction with Other Phytohormones**.
659 *Front Plant Sci* 2017, **8**:475.
660 48. Vaseva, II, Qudeimat E, Potuschak T, Du Y, Genschik P, Vandenbussche F, Van Der
661 Straeten D: **The plant hormone ethylene restricts Arabidopsis growth via the**
662 **epidermis**. *Proc Natl Acad Sci U S A* 2018, **115**(17):E4130-E4139.
663 49. Glick BR: **Bacteria with ACC deaminase can promote plant growth and help to feed**
664 **the world**. *Microbiol Res* 2014, **169**(1):30-39.
665 50. Spaepen S, Vanderleyden J, Remans R: **Indole-3-acetic acid in microbial and**
666 **microorganism-plant signaling**. *FEMS Microbiol Rev* 2007, **31**(4):425-448.
667 51. Spaepen S, Vanderleyden J: **Auxin and plant-microbe interactions**. *Cold Spring Harb*
668 *Perspect Biol* 2011, **3**(4).

669 52. Imada EL, Rolla Dos Santos AA, Oliveira AL, Hungria M, Rodrigues EP: **Indole-3-acetic**
670 **acid production via the indole-3-pyruvate pathway by plant growth promoter**
671 **Rhizobium tropici CIAT 899 is strongly inhibited by ammonium**. *Res Microbiol* 2017,
672 **168**(3):283-292.
673 53. Duca D, Rose DR, Glick BR: **Characterization of a nitrilase and a nitrile hydratase from**
674 **Pseudomonas sp. strain UW4 that converts indole-3-acetonitrile to indole-3-acetic**
675 **acid**. *Appl Environ Microbiol* 2014, **80**(15):4640-4649.
676 54. Duca DR, Rose DR, Glick BR: **Indole acetic acid overproduction transformants of the**
677 **rhizobacterium Pseudomonas sp. UW4**. *Antonie Van Leeuwenhoek* 2018, **111**(9):1645-
678 1660.
679 55. Mayaux JF, Cerbelaud E, Soubrier F, Yeh P, Blanche F, Petre D: **Purification, cloning,**
680 **and primary structure of a new enantiomer-selective amidase from a Rhodococcus**
681 **strain: structural evidence for a conserved genetic coupling with nitrile hydratase**. *J*
682 *Bacteriol* 1991, **173**(21):6694-6704.
683 56. Patten CL, Blakney AJ, Coulson TJ: **Activity, distribution and function of indole-3-acetic**
684 **acid biosynthetic pathways in bacteria**. *Crit Rev Microbiol* 2013, **39**(4):395-415.
685 57. Delamuta JRM, Scherer AJ, Ribeiro RA, Hungria M: **Genetic diversity of Agrobacterium**
686 **species isolated from nodules of common bean and soybean in Brazil, Mexico,**
687 **Ecuador and Mozambique, and description of the new species Agrobacterium**
688 **fabacearum sp. nov**. *Int J Syst Evol Microbiol* 2020, **70**(7):4233-4244.
689 58. Vega-Hernández MC, León-Barrios M, Pérez-Galdona R: **Indole-3-acetic acid**
690 **production from indole-3-acetonitrile in Bradyrhizobium**. *Soil Biology and*
691 *Biochemistry* 2002, **34**(5):665-668.
692 59. Vande Broek A, Lambrecht M, Eggermont K, Vanderleyden J: **Auxins upregulate**
693 **expression of the indole-3-pyruvate decarboxylase gene in Azospirillum brasilense**. *J*
694 *Bacteriol* 1999, **181**(4):1338-1342.
695 60. El-Khawas H, Adachi KJB, Soils Fo: **Identification and quantification of auxins in**
696 **culture media of Azospirillum and Klebsiella and their effect on rice roots**. 1999,
697 **28**(4):377-381.
698 61. Creus CM, Graziano M, Casanovas EM, Pereyra MA, Simontacchi M, Puntarulo S,
699 Barassi CA, Lamattina L: **Nitric oxide is involved in the Azospirillum brasilense-**
700 **induced lateral root formation in tomato**. *Planta* 2005, **221**(2):297-303.
701 62. Molina-Favero C, Creus CM, Simontacchi M, Puntarulo S, Lamattina L: **Aerobic nitric**
702 **oxide production by Azospirillum brasilense Sp245 and its influence on root**
703 **architecture in tomato**. *Mol Plant Microbe Interact* 2008, **21**(7):1001-1009.
704 63. Steenhoudt O, Keijers V, Okon Y, Vanderleyden J: **Identification and characterization**
705 **of a periplasmic nitrate reductase in Azospirillum brasilense Sp245**. *Arch Microbiol*
706 2001, **175**(5):344-352.
707 64. Bethke PC, Badger MR, Jones RL: **Apoplastic synthesis of nitric oxide by plant tissues**.
708 *Plant Cell* 2004, **16**(2):332-341.
709 65. Molina-Favero C, Mónica Creus C, Lanteri ML, Correa-Aragunde N, Lombardo MC,
710 Barassi CA, Lamattina L: **Nitric Oxide and Plant Growth Promoting Rhizobacteria:**
711 **Common Features Influencing Root Growth and Development**. In: *Advances in*
712 *Botanical Research.* vol. 46: Academic Press; 2007: 1-33.

713 66. Zhang Y, Burris RH, Ludden PW, Roberts GP: **Regulation of nitrogen fixation in**
714 **Azospirillum brasilense**. *FEMS Microbiol Lett* 1997, **152**(2):195-204.
715 67. Malinich EA, Bauer CE: **Transcriptome analysis of Azospirillum brasilense vegetative**
716 **and cyst states reveals large-scale alterations in metabolic and replicative gene**
717 **expression**. *Microb Genom* 2018, **4**(8).
718 68. Lecomte SM, Achouak W, Abrouk D, Heulin T, Nesme X, Haichar FeZ: **Diversifying**
719 **Anaerobic Respiration Strategies to Compete in the Rhizosphere**. 2018, **6**(139).
720 69. Fujisaki S, Ohnuma S, Horiuchi T, Takahashi I, Tsukui S, Nishimura Y, Nishino T,
721 Kitabatake M, Inokuchi H: **Cloning of a gene from Escherichia coli that confers**
722 **resistance to fosmidomycin as a consequence of amplification**. *Gene* 1996, **175**(1-
723 2):83-87.
724 70. Bentley J, Hyatt LS, Ainley K, Parish JH, Herbert RB, White GR: **Cloning and sequence**
725 **analysis of an Escherichia coli gene conferring bicyclomycin resistance**. *Gene* 1993,
726 **127**(1):117-120.
727 71. El Ghachi M, Bouhss A, Blanot D, Mengin-Lecreulx D: **The bacA gene of Escherichia coli**
728 **encodes an undecaprenyl pyrophosphate phosphatase activity**. *J Biol Chem* 2004,
729 **279**(29):30106-30113.
730 72. Anzai H, Yoneyama K, Yamaguchi I: **The nucleotide sequence of tabtoxin resistance**
731 **gene (ttr) of Pseudomonas syringae pv. tabaci**. *Nucleic Acids Res* 1990, **18**(7):1890.
732 73. Giddens SR, Feng Y, Mahanty HK: **Characterization of a novel phenazine antibiotic**
733 **gene cluster in Erwinia herbicola Eh1087**. *Mol Microbiol* 2002, **45**(3):769-783.
734 74. Waters SH, Rogowsky P, Grinsted J, Altenbuchner J, Schmitt R: **The tetracycline**
735 **resistance determinants of RP1 and Tn1721: nucleotide sequence analysis**. *Nucleic*
736 *Acids Res* 1983, **11**(17):6089-6105.
737 75. Nagakubo S, Nishino K, Hirata T, Yamaguchi A: **The putative response regulator BaeR**
738 **stimulates multidrug resistance of Escherichia coli via a novel multidrug exporter**
739 **system, MdtABC**. *J Bacteriol* 2002, **184**(15):4161-4167.
740 76. Okusu H, Ma D, Nikaido H: **AcrAB efflux pump plays a major role in the antibiotic**
741 **resistance phenotype of Escherichia coli multiple-antibiotic-resistance (Mar)**
742 **mutants**. *J Bacteriol* 1996, **178**(1):306-308.
743 77. Brown MH, Paulsen IT, Skurray RA: **The multidrug efflux protein NorM is a prototype**
744 **of a new family of transporters**. *Mol Microbiol* 1999, **31**(1):394-395.
745 78. Vior NM, Lacret R, Chandra G, Dorai-Raj S, Trick M, Truman AW: **Discovery and**
746 **Biosynthesis of the Antibiotic Bicyclomycin in Distantly Related Bacterial Classes**.
747 *Appl Environ Microbiol* 2018, **84**(9).
748 79. Abdelfattah MS, Ishikawa N, Karmakar UK, Yamaku K, Ishibashi M: **New phenazine**
749 **analogues from Streptomyces sp. IFM 11694 with TRAIL resistance-overcoming**
750 **activities**. *J Antibiot (Tokyo)* 2016, **69**(6):446-450.
751 80. Procopio RE, Silva IR, Martins MK, Azevedo JL, Araujo JM: **Antibiotics produced by**
752 **Streptomyces**. *Braz J Infect Dis* 2012, **16**(5):466-471.
753 81. Chater KF, Biro S, Lee KJ, Palmer T, Schrempf H: **The complex extracellular biology of**
754 **Streptomyces**. *FEMS Microbiol Rev* 2010, **34**(2):171-198.
755 82. Chater KF: **Recent advances in understanding Streptomyces**. *F1000Res* 2016, **5**:2795.

756 83. Bramwell PA, Barallon RV, Rogers HJ, Bailey MJ: **Extraction and PCR amplification of**
757 **DNA from the rhizoplane**. In: *Molecular microbial ecology manual.* Springer; 1995: 89-
758 108.
759 84. Baldani JI, Reis VM, Videira SS, Boddey LH, Baldani VLD: **The art of isolating nitrogen-**
760 **fixing bacteria from non-leguminous plants using N-free semi-solid media: a practical**
761 **guide for microbiologists**. *Plant and Soil* 2014, **384**(1):413-431.
762 85. Poly F, Ranjard L, Nazaret S, Gourbiere F, Monrozier LJ: **Comparison of nifH gene pools**
763 **in soils and soil microenvironments with contrasting properties**. *Appl Environ*
764 *Microbiol* 2001, **67**(5):2255-2262.
765 86. Kumar V, Narula N: **Solubilization of inorganic phosphates and growth emergence of**
766 **wheat as affected by Azotobacter chroococcum mutants**. *Biology and Fertility of Soils*
767 1999, **28**(3):301-305.
768 87. Intorne AC, de Oliveira MV, Lima ML, da Silva JF, Olivares FL, de Souza Filho GA:
769 **Identification and characterization of Gluconacetobacter diazotrophicus mutants**
770 **defective in the solubilization of phosphorus and zinc**. *Arch Microbiol* 2009,
771 **191**(5):477-483.
772 88. Sarwar M, Kremer RJ: **Determination of bacterially derived auxins using a microplate**
773 **method**. *Letters in Applied Microbiology* 1995, **20**(5):282-285.
774 89. Baldotto LEB, Olivares FL, Bressan-Smith R: **Structural interaction between GFP-**
775 **labeled diazotrophic endophytic bacterium Herbaspirillum seropedicae RAM10 and**
776 **pineapple plantlets 'Vitória'**. *Brazilian Journal of Microbiology* 2011, **42**:114-125.
777 90. Bolger AM, Lohse M, Usadel B: **Trimmomatic: a flexible trimmer for Illumina**
778 **sequence data**. *Bioinformatics* 2014, **30**(15):2114-2120.
779 91. Bankevich A, Nurk S, Antipov D, Gurevich AA, Dvorkin M, Kulikov AS, Lesin VM,
780 Nikolenko SI, Pham S, Prjibelski AD *et al*: **SPAdes: a new genome assembly algorithm**
781 **and its applications to single-cell sequencing**. *J Comput Biol* 2012, **19**(5):455-477.
782 92. Gurevich A, Saveliev V, Vyahhi N, Tesler G: **QUAST: quality assessment tool for**
783 **genome assemblies**. *Bioinformatics* 2013, **29**(8):1072-1075.
784 93. Tatusova T, DiCuccio M, Badretdin A, Chetvernin V, Nawrocki EP, Zaslavsky L,
785 Lomsadze A, Pruitt KD, Borodovsky M, Ostell J: **NCBI prokaryotic genome annotation**
786 **pipeline**. *Nucleic acids research* 2016, **44**(14):6614-6624.
787 94. O'Leary NA, Wright MW, Brister JR, Ciufo S, Haddad D, McVeigh R, Rajput B, Robbertse
788 B, Smith-White B, Ako-Adjei D *et al*: **Reference sequence (RefSeq) database at NCBI:**
789 **current status, taxonomic expansion, and functional annotation**. *Nucleic Acids Res*
790 2016, **44**(D1):D733-745.
791 95. Pruitt KD, Tatusova T, Maglott DR: **NCBI reference sequences (RefSeq): a curated non-**
792 **redundant sequence database of genomes, transcripts and proteins**. *Nucleic Acids*
793 *Res* 2007, **35**(Database issue):D61-65.
794 96. Seemann T: **Prokka: rapid prokaryotic genome annotation**. *Bioinformatics* 2014,
795 **30**(14):2068-2069.
796 97. Altschul SF, Madden TL, Schaffer AA, Zhang J, Zhang Z, Miller W, Lipman DJ: **Gapped**
797 **BLAST and PSI-BLAST: a new generation of protein database search programs**.
798 *Nucleic Acids Res* 1997, **25**(17):3389-3402.

98. Pritchard L, Glover RH, Humphris S, Elphinstone JG, Toth IK: **Genomics and taxonomy in diagnostics for food security: soft-rotting enterobacterial plant pathogens**. *Analytical Methods* 2016, **8**(1):12-24.
99. Page AJ, Cummins CA, Hunt M, Wong VK, Reuter S, Holden MT, Fookes M, Falush D, Keane JA, Parkhill J: **Roary: rapid large-scale prokaryote pan genome analysis**. *Bioinformatics* 2015, **31**(22):3691-3693.
100. Edgar RC: **MUSCLE: multiple sequence alignment with high accuracy and high throughput**. *Nucleic Acids Res* 2004, **32**(5):1792-1797.
101. Stamatakis A: **RAxML version 8: a tool for phylogenetic analysis and post-analysis of large phylogenies**. *Bioinformatics* 2014, **30**(9):1312-1313.

844 **FIGURES**

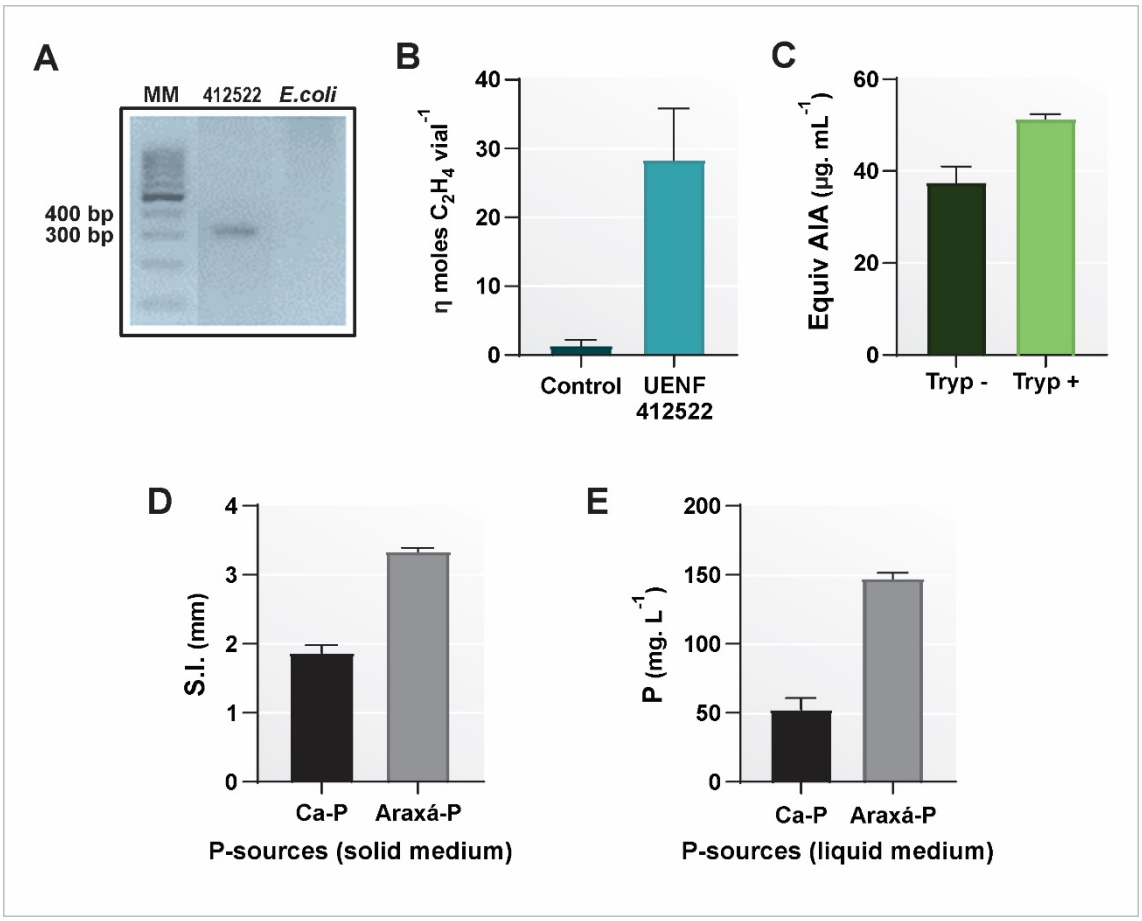


845

846 **Figure 1:** Plant growth promotion *in vitro* traits of *Azospirillum* sp. UENF-412522. (A)
847 Amplification of *nifH* using *E. coli* as negative control; molecular weight marker (MM). (B)
848 Nitrogenase activity by the acetylene reduction assay. (C) Indole acetic acid (IAA) production
849 with and without L- tryptophan. Araxá P-rock and calcium phosphate solubilization in solid (D)
850 and liquid (E) medium.

851

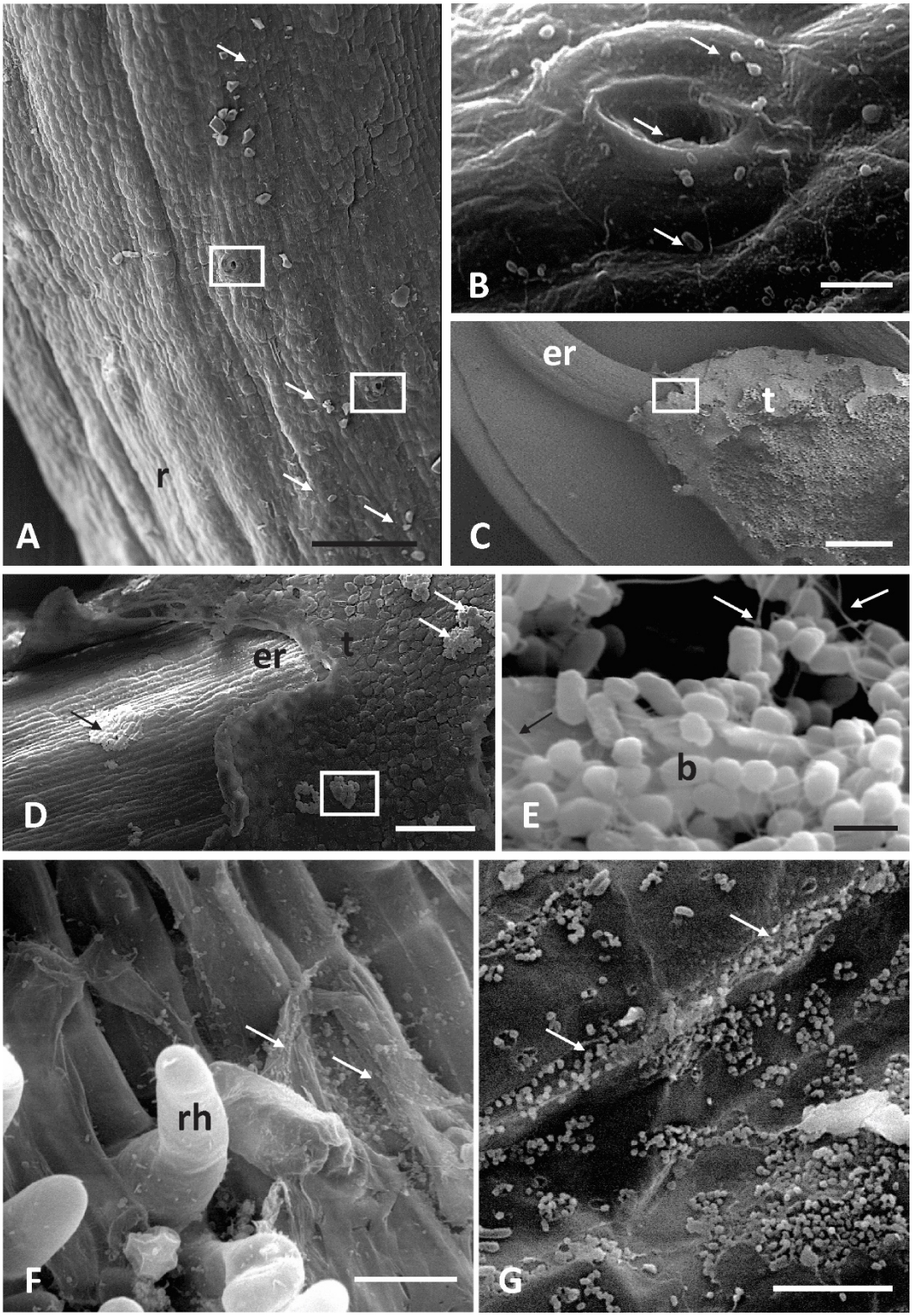


**Figure 2:** Scanning electron microscopy (SEM) of passion fruit (*Passiflora edulis* subsp. *edulis*) seed to seedlings phase inoculated with *Azospirillum* sp. UENF-412522 in an axenic cultivation system at one day (A-E) and seven days after germination (F-G). (A) General view of the emerged radicle surface (r) with single bacteria cells attached (arrows). Note the sparse rudimentary stomata (rectangle magnified in B), bar = 100 µm; (B) Bacteria cells in the vicinity and into the stomata pore (arrows), bar = 5µm; (C) General view of the emerged radicle (er) breaking the seed tegument (t), rectangle magnified in D, bar = 1000 µm; (D) Transition zone between broken

tegument (t) and emerged radicle with bacterial aggregates visible in surface tegument (white arrows) and emerged roots (black arrow), rectangle magnified in E, bar = 100 µm; (E) Bacteria aggregates (b) attached by fibrils in the seed surface (black arrow) and linking cell-to-cell (white arrows), bar = 1 µm; (F) Bacteria cells colonizing the root hair (rh) zone as a single-cell by apolar attachment, bar = 20 µm; (G) Aggregated bacteria cells colonizing the elongation-differentiation root zone mainly by apolar attachment and associated to the epidermal cell-wall-junction, bar = 10 µm.

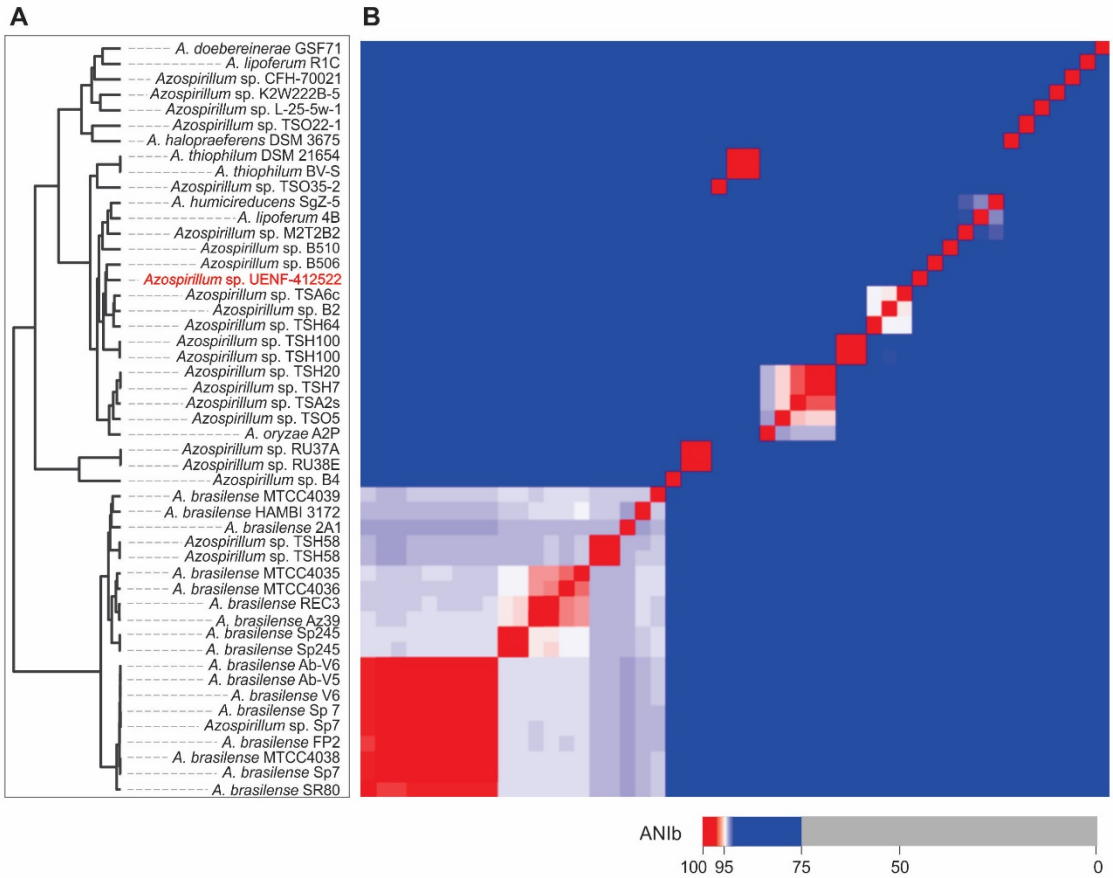


**Figure 3:** Average nucleotide identity (ANI). (A) Neighbor-joining cladogram. (B) Genome-to-genome distance matrix.

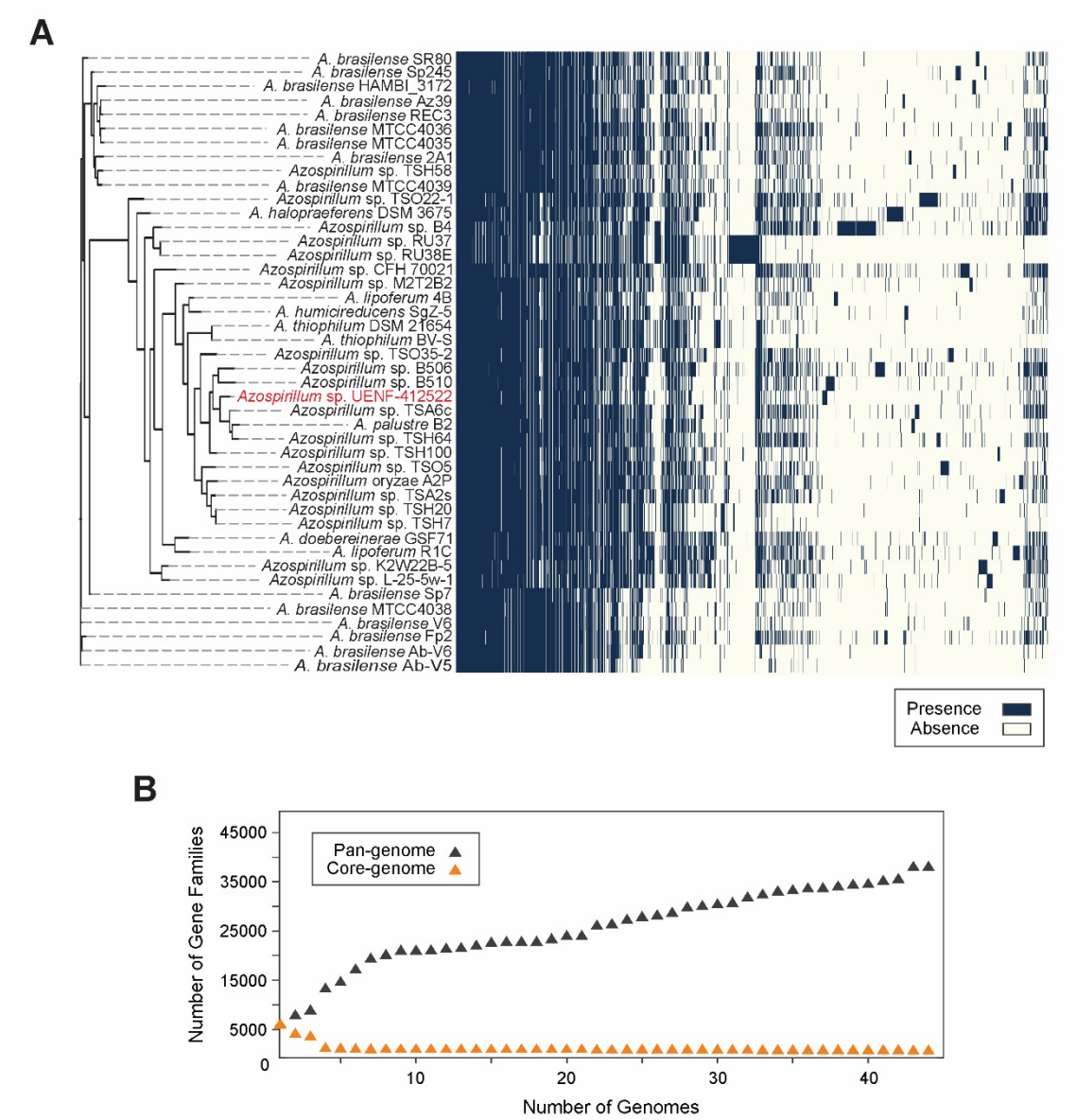


**Figure 4:** *Azospirillum* spp. pan-genome. (A) Gene presence/absence matrix, with gene presence depicted with solid blue boxes. (B) Pan- and core-genome sizes versus new genomes additions to the pan-genome dataset.

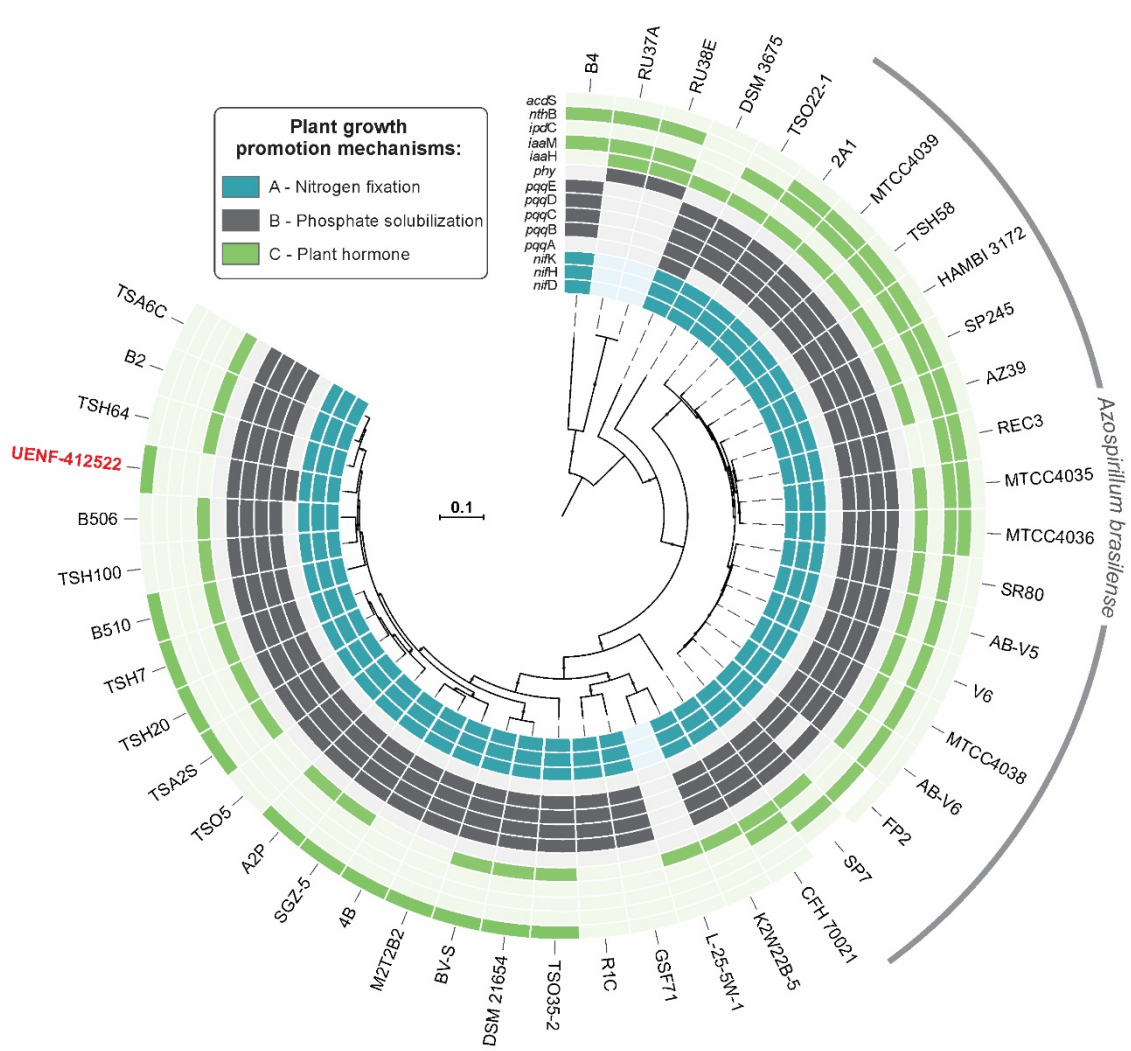


**Figure 5:** Core maximum likelihood phylogenetic tree. Plant growth-promoting genes were searched, grouped according to the mechanism of growth modulation, and mapped onto the tree.

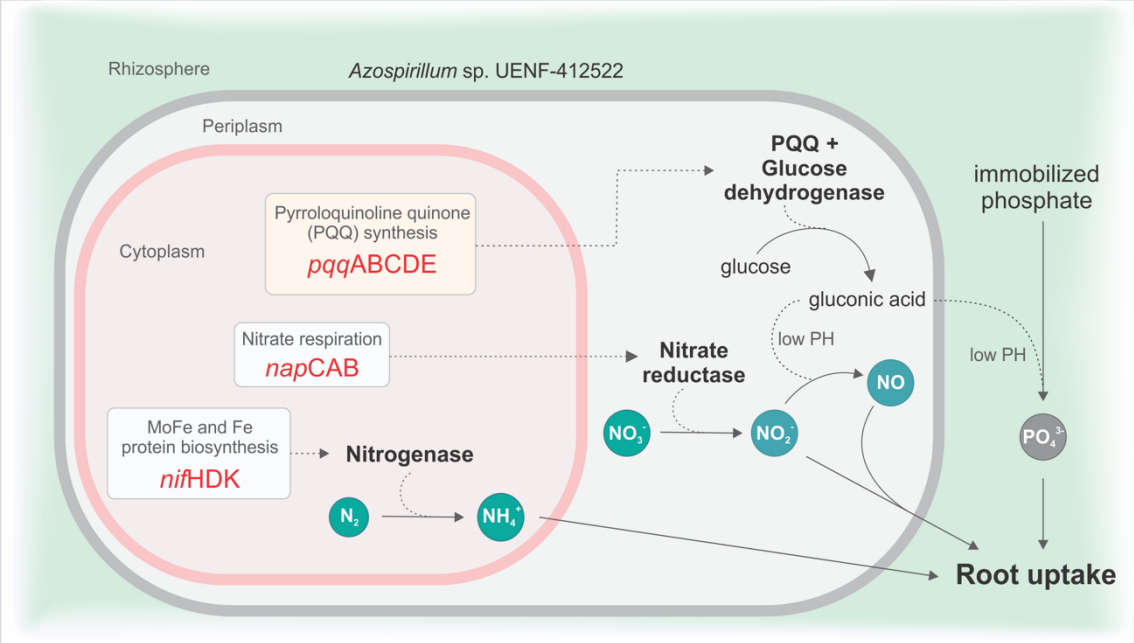


**Figure 6**: Schematic representation of nitrogen fixation, phosphate solubilization, and nitrite/nitric oxide emission by *Azospirillum sp.* UENF-412522 in the rhizosphere. The identified genes responsible for nitrogen fixation (*nifHDK*), root enhancement (*napCAB*), and phosphate solubilization (*pqqABCDE*) are represented within boxes. Nitrogen fixation occurs in the cytoplasm, while gluconic acid production and nitrate respiration take place at the periplasm. Ammonium generated by the nitrogenase can undergo anaerobic nitrification to nitrite, which can be exported to the periplasm. In the periplasm, glucose dehydrogenase, along with the PQQ co-factor, produces gluconic acid from glucose, lowering the pH. Nitrate is reduced to nitrite by a periplasmatic nitrate reductase napCAB. At low pH, nitrite can be reduced to nitric oxide. Acetic acid, nitrite, and nitric oxide can be exported to the rhizosphere. Acetic acid can reduce the pH in the rhizosphere and solubilize phosphate. The solubilized phosphate, nitrite, and nitric oxide can be captured by root cells.